The Journal of Infectious Diseases

MAJOR ARTICLE

Zika Virus Replicates in Proliferating Cells in Explants From First-Trimester Human Placentas, Potential Sites for Dissemination of Infection

Takako Tabata,[1,a] Matthew Petitt,[1,a] Henry Puerta-Guardo,[2] Daniela Michlmayr,[2] Eva Harris,[2] and Lenore Pereira[1]

[1]Department of Cell and Tissue Biology, School of Dentistry, University of California San Francisco; and [2]Division of Infectious Disease and Vaccinology, School of Public Health, University of California Berkeley

Background. Maternal Zika virus (ZIKV) infection with prolonged viremia leads to fetal infection and congenital Zika syndrome. Previously, we reported that ZIKV infects primary cells from human placentas and fetal membranes. Here, we studied viral replication in numerous explants of anchoring villi and basal decidua from first-trimester human placentas and midgestation amniotic epithelial cells (AmEpCs).

Methods. Explants and AmEpCs were infected with American and African ZIKV strains at low multiplicities, and ZIKV proteins were visualized by immunofluorescence. Titers of infectious progeny, cell proliferation, and invasiveness were quantified.

Results. In anchoring villus, ZIKV replicated reproducibly in proliferating cytotrophoblasts in proximal cell columns, dividing Hofbauer cells in villus cores, and invasive cytotrophoblasts, but frequencies differed. Cytotrophoblasts in explants infected by Nicaraguan strains were invasive, whereas those infected by prototype MR766 largely remained in cell columns, and titers varied by donor and strain. In basal decidua, ZIKV replicated in glandular epithelium, decidual cells, and immune cells. ZIKV-infected AmEpCs frequently occurred in pairs and expressed Ki67 and phosphohistone H3, indicating replication in dividing cells.

Conclusions. ZIKV infection in early pregnancy could target proliferating cell column cytotrophoblasts and Hofbauer cells, amplifying infection in basal decidua and chorionic villi and enabling transplacental transmission.

Keywords. Zika virus; placenta; decidua; congenital infection.

Zika virus (ZIKV) is a mosquito-borne flavivirus responsible for the 2015–2017 pandemic in the Americas. ZIKV infection during pregnancy is associated with devastating birth defects designated congenital Zika syndrome (CZS), which includes microcephaly, neurological impairment, cerebral calcification, and retinal damage [1–5]. Over 2700 CZS cases have been reported in 207 000 confirmed maternal infections (incidence 1.3%) during ZIKV epidemics in the Americas in 2015–2017 [6]. ZIKV RNA has been found in the brain, placenta, and amniotic fluid of infected babies and in maternal blood for prolonged periods in cases of congenital infection [3, 7, 8]. ZIKV was first isolated in 1947 in an African forest but epidemics in the South Pacific and the Americas that caused human disease were first reported in 2007 and 2015, respectively, and may be associated with adaptations to the human host [9, 10].

How ZIKV crosses the placental barrier and reaches the fetus is unknown. We reported that the African prototype ZIKV strain MR766 and American strains from Nicaragua (Nica1-16 and Nica2-16) infect primary cells isolated from human placentas and amniochorionic membranes and replicate in anchoring villus explants producing infectious progeny [11]. In addition, human T-cell immunoglobulin and mucin-domain containing protein 1 (TIM1), uniformly detected in human placentas, functions as a membrane cofactor for ZIKV infection. We found that infected villus explants express the ZIKV nonstructural protein 3 (NS3) and envelope protein (E) in cytotrophoblasts (CTBs) of proximal cell columns and in Hofbauer cells (fetal macrophages) in the villus core, but overlying syncytiotrophoblasts (STBs) are not infected. These results suggest that ZIKV spreads from maternal circulation to basal decidua and chorionic villi in the interstitial blood space and to amniochorionic membranes in contact with parietal decidua [11].

Trophoblasts, important targets of ZIKV infection in human placentas, differentiate by fusing into STBs or remain single CTBs that invade the uterine wall and vasculature, thereby anchoring the placenta to the uterus and accessing the maternal blood supply. At the tips of chorionic villi, CTBs proliferate forming proximal cell columns that are suspended in the maternal blood space [12, 13]. In distal columns, CTBs differentiate into an endothelial phenotype, invade decidua, and remodel uterine blood vessels. To facilitate these functions, CTBs

Received 23 August 2017; editorial decision 4 October 2017; accepted 17 October 2017; published online November 2, 2017.

Presented in part: A portion of this work was presented at the Annual Meeting of the Society for Reproductive Investigation, Orlando FL, March 2017.

[a]These authors contributed equally.

Correspondence: L. Pereira, PhD, Department of Cell and Tissue Biology, University of California, San Francisco, San Francisco, CA 94143, USA (lenore.pereira@ucsf.edu).

The Journal of Infectious Diseases® 2018;217:1202–13

DOI: 10.1093/infdis/jix552

upregulate key integrins α1β1 and αvβ3, secrete matrix metalloproteinase MMP-9, and express MHC class I molecule HLA-G [14–16]. Throughout development, placentas form branching villi from proliferating CTB sprouts that increase in size by infiltration of mesenchymal cells and vascularization [17].

Here, we analyzed ZIKV replication in explants of chorionic villus, basal decidua, and midgestation amniotic epithelial cells (AmEpCs) at low multiplicities of infection to simulate natural levels of viremia during pregnancy [18]. ZIKV proteins were detected in cell column and invasive CTBs and Hofbauer cells in villus cores, and virus replicated in glandular epithelium, decidual cells, and immune cells in basal decidua. Analysis of anchoring villus explants indicated that CTBs infected with the Nicaraguan ZIKV strains differentiated and invaded the extracellular matrix, whereas cells infected with the prototype Uganda strain MR766 were largely impaired in invasion. Detection of infection by African and American strains in paired neighbor cells and costaining for markers of cell proliferation showed that infected cells continue to divide. Our results suggest that ZIKV replication in basal decidua and chorionic villi could lead to prolonged infection and increase the viral load in the maternal blood space, contributing to transplacental transmission in the first trimester of gestation.

MATERIALS AND METHODS

ZIKV Strains and Infection

Prototype (Uganda 1947, MR766; resequenced, GenBank accession KX421193), Dakar41519 isolated in 1984 from mosquitoes in Senegal, and Puerto Rico PRVABC59 strains were a gift from Michael S. Diamond (Washington University, St. Louis). Nica1-16 and Nica2-16 (GenBank accession KX421195 and KX421194) were isolated from ZIKV-infected patients (National Virology Laboratory, Ministry of Health, Managua, Nicaragua), propagated in C6/36 cells and used at low passage [11]. Cell-free supernatants were harvested 3 days postinfection (dpi) and stored at −80°C.

Infection of Placental Villus and Decidua Explants

The Institutional Review Board of the University of California San Francisco approved this study. Anchoring villi were prepared from placentas (1 at 7.5 weeks, 2 at 8 weeks, 2 at 10 weeks, and 2 at 11 weeks' gestation) and attached basal decidua (8 and 11 weeks' gestation) from elective terminations (Advanced Bioscience Resources). Chorionic villi were isolated and cultured on Millicell-CM inserts (0.4 μm pore size, 12 mm, Millipore) coated with Matrigel [11]. Twenty hours after attachment, explants were rinsed with fresh medium, infected with ZIKV MR766, Nica1-16, or Nica2-16 (5×10^4 focus forming units [FFU]/explant) overnight and maintained for 3 days [11, 19]. Four decidua explants (approximately 2–4 mm) were plated on Matrigel-coated inserts (30 mm) and cultured in 96.5% Dulbecco's Modified Eagle's Medium (DME) H-21 with 2.5% fetal bovine serum (FBS).

Amniotic Epithelial Cell Isolation, Culture, and Infection

Primary AmEpCs were isolated from membranes at 19.4 and 21.2 weeks' gestational age and cultured as published [11, 20]. ARPE-19 cells were grown in DMEM (Gibco) supplemented with 10% FBS. AmEpCs (passage 1) were infected with MR766, Nica1-16, Nica2-16, Dakar41519, and PRVABC59 at multiplicities of infection (MOI) of 0.003–0.03.

Antibodies and Reagents

Commercial antibodies were: rabbit polyclonal anti-TIM1 and anti-Ki67, and mouse monoclonal anti-Ki67 (Abcam); anti-CD68 and cytokeratin 7 mouse mAb (Dako); rabbit polyclonal anti-ZIKV proteins (E) (GeneTex); and rabbit monoclonal antiphosphohistone H3 (Ser10) (Cell Signaling Technology). Rat anti-human cytokeratin mAb (clone 7D3) reactive with trophoblasts was a gift from Susan Fisher (University of California San Francisco) [21]. Anti-DENV nonstructural protein 3 (NS3) mAb E1D8 was generated by the Harris laboratory [22]. Antienvelope (E) mAb 4G2 was obtained from the American Type Culture Collection.

ZIKV Titration

Titers were determined by immunofluorescence-based focus-forming assay in ARPE-19 cells [11] using mAb 4G2 [23].

Immunofluorescence Staining

Cells or tissue sections were incubated with primary antibodies and secondary antibodies labeled with fluorescein isothiocyanate (FITC), rhodamine red-X (RRX), or Cy5 (Jackson ImmunoResearch). Nuclei were counterstained with 4',6-diamidino-2-phenylindole (DAPI; Vector Laboratories). Images were obtained using a Nikon Eclipse 50i microscope with a SPOT 7.4 Slider camera (Diagnostic Instruments) controlled by Spot advanced software or using a Leica DMi8 microscope with a Leica DFC9000GT camera controlled by Leica Application Suite X software.

RESULTS

ZIKV Replicates at Consistent Sites in Explants of First-Trimester Placentas

In an anchoring villus explant grown on Matrigel, villus cores are surrounded by CTBs in cell columns and outgrowths of invasive cells (Figure 1A*i*). The diagram illustrates villus architecture, direction of CTB migration from the cell column, and how sectioning planes capture villus cores, proximal cell columns, and invasive CTBs (Figure 1A*ii*). Sections immunostained for cytokeratin 7 (CK), expressed by CTBs, shows villus cores and proliferating CTBs in proximal cell columns, a branching villus, and zones of invasive CTBs surrounding cell columns (Figure 1B). To identify ZIKV-infected cells, explants were infected with Nica2-16, fixed

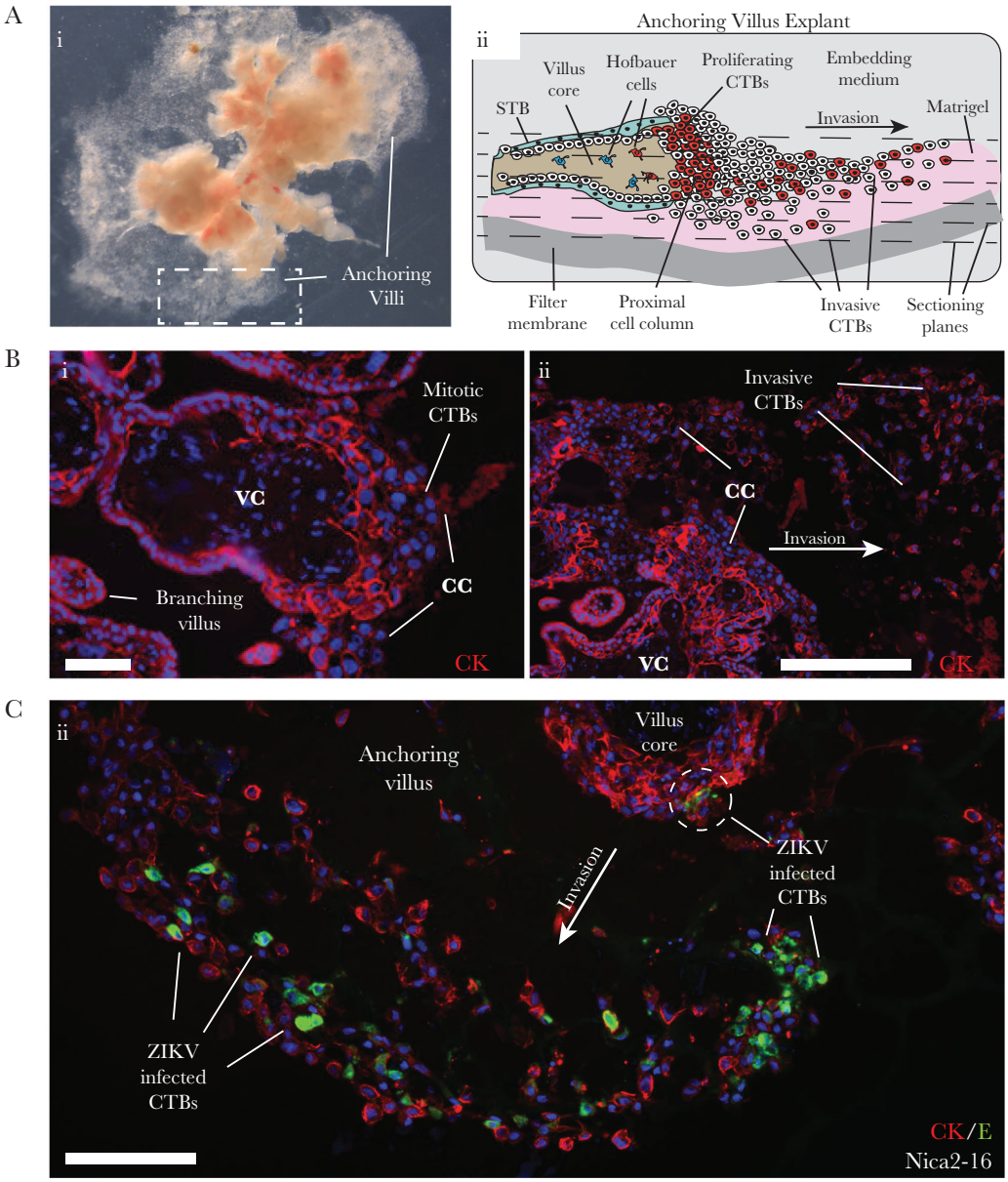

Figure 1. Anchoring villus explant model of ZIKV infection in first-trimester human placentas. *Ai*, Explant of an anchoring chorionic villus at 4 days after attachment and 3 days postinfection (dpi). Virus inoculum was added 24 hours after explants were dissected and plated on Matrigel, an extracellular matrix of laminin and collagen, and removed 24 hours later. White rectangle indicates an area of active cytotrophoblast (CTB) invasion corresponding to immunostained section in (*C*). *Aii*, Diagram of anchoring chorionic villus explant plated on Matrigel-coated Transwell filter 3–4 days after plating with extensive CTB invasion. Explants were embedded, frozen, and sectioned in the planes indicated. *B*, Villus explant sections immunostained for the CTB marker cytokeratin 7 (CK) identifying cell columns (CC) and invasive CTBs. *C*, Anchoring villus section immunostained for ZIKV E protein and CK at 3 dpi. Dashed circle indicates a focus of infection in a cell column, where CTBs proliferate. Scale bars = 100 µm. Explants in panels (*A*) and (*C*) were from placenta #1 (8 weeks' gestation).

at 3 dpi and immunostained for ZIKV E and NS3. A section of a villus explant shows a focal site of infected CTBs proximal to the villus core and a broad zone of invasive CTBs (Figure 1C). In the invasion zone, approximately 25% of CTBs were infected and intermingled with uninfected CK-positive cells. These results show that Nica2-16–infected CTBs differentiate and invade together with uninfected cells.

Figure 2 illustrates the 3 sites of ZIKV infection consistently observed in anchoring villi (n = 180) from 6 first-trimester placentas: CTBs in proximal columns of proliferating cells, CTBs within zones of differentiating/invasive cells, and Hofbauer cells, often as pairs, in villus cores. At the first site, a focus of ZIKV MR766 infection contained 5 pairs of infected CTBs in a proximal cell column at 3 dpi (Figure 2A*i*; enlargement in Figure 2C*i*), and a Nica1-16–infected villus contained 3 pairs of infected CTBs in a proximal cell column at 1 dpi (Figure 2A*ii*). At the second site, shown in a Nica2-16–infected villus, CTBs were detected in a zone of differentiating/invasive cells at

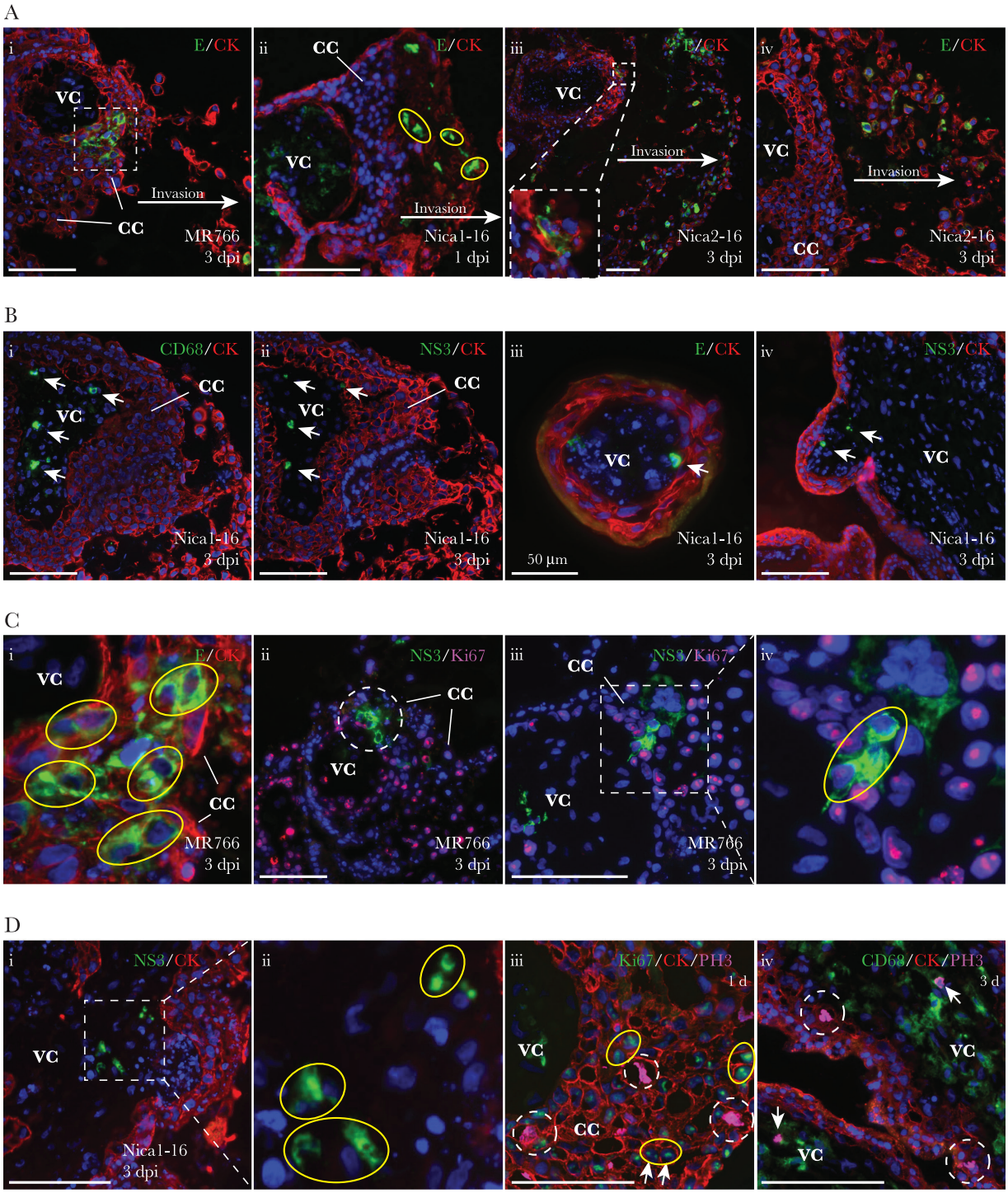

Figure 2. Consistent sites of ZIKV infection in anchoring villus explants. *A*, Villus explants infected with MR766 (*i*), Nica1-16 (*ii*), or Nica2-16 (*iii, iv*) and immunostained for cytokeratin 7 (CK) and ZIKV E protein at 1 or 3 days postinfection (dpi). Typical images of infected cells selected from n = 180 villi from 6 placentas. *B*, Nica1-16–infected explants immunostained for CK and CD68 (*i*), ZIKV NS3 (*ii* and *iv*), or E protein (*iii*). *Ci*, Magnification of cell column (CC) area from (*Ai*) (dashed square). *Cii–iv*, MR766-infected villus explants immunostained for NS3 and Ki67. *Di, ii*, Nica1-16–infected villus explant immunostained for CK and NS3. *Diii, iv*, Uninfected villus explants immunostained for CK, phosphohistone H3 (PH3), and either Ki67 (*iii*) or CD68 (*iv*). Dashed circles indicate cells in M phase based on PH3 signal. Yellow circles in all panels indicate pairs of infected cells (*Aii, Ci, Civ, Dii*) or proliferating cells (*Diii*). Except as indicated in (*Biii*), scale bars = 100 µm. Abbreviation: VC, villus core.

3 dpi, intermingled with CK-positive uninfected cells (Figure 2A*iii,iv*). However, in an MR766-infected villi, infected CTBs in cell columns failed to become invasive (Figure 2C*i–iv*). At the third site of infection, Hofbauer cells expressing NS3 and E were observed in cores of Nica1-16–infected villi (Figure 2B*i,ii*), small branching villi (Figure 2B*iii*), and sprouts (Figure 2B*iv*).

Next, we showed that ZIKV-infected cells proliferate by immunostaining phosphohistone 3 (PH3), indicating M phase, and Ki67, indicating active proliferation. In proximal cell columns, MR766-infected CTBs were found in pairs (Figure 2C*i*), suggesting they arose from division of single infected cells. Also, pairs of NS3-expressing cells occurred in areas with Ki67-positive cells and often continued to express Ki67 (Figure 2C*ii–iv*). Likewise, 3 pairs of dividing NS3-expressing Hofbauer cells were found in the villus core of a Nica1-16–infected explant (Figure 2D*i,ii*). The configurations of infected CTBs in proximal cell columns and Hofbauer cells in villus cores resembled those of proliferating cells in control explants. CTBs expressing PH3 were found among many Ki67-positive cells in a proximal column (Figure 2D*iii*), and PH3-positive CTBs and nearby Hofbauer cells were present in adjacent villi (Figure 2D*iv*). A survey of 7 MR766- and Nica-infected explants showed that 14 pairs of infected CTBs were in proximal cell columns and 5 pairs still expressed Ki67 at 3 dpi. Although far fewer Nica2-16–infected CTBs were found in proximal cell columns, these occurred in pairs at 1 dpi (Figure 2A*ii*); however, the villi contained predominately invasive infected CTBs at 3 dpi (Figure 2A*iii,iv*). Together, these results showed that both ZIKV strains replicate in proliferating CTBs in proximal cell columns and Hofbauer cells in villus cores, but that Nicaraguan strains also replicate in invasive CTBs.

We then infected anchoring villi alongside floating villi, which mostly lack cell columns and invasive CTBs. Analysis of 45 floating villi from placenta 5 indicated that only occasional truncated cell columns developed, proliferating CTBs were rare, and few were infected (Figure 3A*i,ii*). When Hofbauer cells were infected, single cells or pairs were found near breaks in surface STBs (Figure 3A*iii,iv*). In contrast, anchoring villi contained invasive CTBs expressing E protein alongside many uninfected CK-positive CTBs (Figure 3B*i*) and a pair of infected Hofbauer cells near proliferating CTBs in proximal cell columns (Figure 3B*ii*). Further, we found that Nica-2-16–infected floating villi produced low titers, averaging 40–60 FFU/mL, whereas titers from anchoring villi from placenta 5 were considerably higher (Supplementary Figure S1). These results confirmed that the Nicaraguan ZIKV strains replicate in cell-column CTBs and invasive CTBs and suggests that the low virus output from floating villus explants is due to the absence of these target cells.

To determine whether the adjacent basal decidua could serve as a source of infectious ZIKV released into the maternal blood space, decidua explants were infected with Nicaraguan strains and prototype MR766. Glandular epithelia were most frequently infected and expressed ZIKV E protein, which was also detected in flanking decidual and dendritic cells (Figure 4D*i–v*). Titration of infectious progeny showed that Nicaraguan ZIKV strains produced higher virus titers than MR766-infected decidua (Supplementary Figure S1).

Table 1 summarizes the sites of infection in 355 sections of anchoring villi representing 180 villi from 6 first-trimester infected placentas. We observed infected cells expressing ZIKV E or NS3 proteins in: (1) proliferating CTBs in proximal cell columns (Nica [12%] vs MR766 [39%]); (2) zones of differentiating/invasive CTBs (Nica [55%] vs MR766 [7%]); and (3) Hofbauer cells in villus cores (Nica [37%] vs MR766 [24%]). The frequencies of infection depended primarily on the ZIKV strain. Nica1-16–infected villi from placentas 1, 3, and 4 contained infected invasive CTBs in 89%, 50%, and 67%, respectively, and produced the highest titers (Supplementary Table S1). In MR766-infected explants, cell columns were most frequently infected (39%) but not invasive CTBs (7%). Hence, placentas 6 and 7, which contained few villi with infected invasive CTBs, produced lower virus titers (Supplementary Figure S1). Hofbauer cell infection was more frequent in Nica-infected (37%) than MR766-infected (24%) villi, and was higher in placentas 3, 4, and 5, which were collected close to the end of first trimester, when Hofbauer cell density increases [24]. Notably, Hofbauer cell infection was independent of nearby CTB infection, suggesting that virus spread does not require cell–cell contact (Figure 2B*i–iv,* D*i,ii*). Together, these results show consistent sites of ZIKV replication in proliferating CTBs and Hofbauer cells in villus cores and zones of invasive CTBs, with frequencies that vary by strain and gestational age. Moreover, ZIKV replicates in basal decidua, targeting glandular epithelium and decidual cells, suggesting that the adjacent decidua could amplify the viral load.

Nica-Infected CTBs Differentiate/Invade But Cells Infected With MR766 Prototype ZIKV Are Impaired

Table 1 indicated differences in the ability of MR766- and Nica-infected CTBs to become invasive cells. Detailed comparison of CTBs in MR766-infected villi showed that few infected CTBs left the proximal cell columns to invade the extracellular matrix, although many uninfected CK-positive CTBs were invasive (Figure 5A*i,ii*). However, in Nica-infected villi, many E- and NS3-expressing CTBs invaded alongside uninfected cells (Figure 1C, Figure 5A*iii,iv*). Scale bars of 100 µm (Figure 5A*i,ii*) and 400 µm (Figure 5A*iii,iv*) for the MR766- and Nica1-16–infected villi, respectively, indicate significantly greater average invasion distance by the Nica1-16–infected cells. We then measured invasion distances for all infected cells in 30 anchoring villi (15 each for Nica and MR766) and calculated an average migration distance (Figure 5B). The average of all invasion distances for Nica-infected CTBs was 350 µm and MR766-infected CTBs was 60 µm, indicating that Nica-infected cells were 6 times more invasive. Only 4 Nica-infected CTBs failed to leave cell columns, but as many as 83 MR766-infected CTBs did not invade (Figure 5B, circled numbers). Occasionally, infected CTBs fragmented at short distances from villus cores, but differences between strains were not significant (not shown). These data show that CTBs infected with Nicaraguan strains differentiate and invade side-by-side with uninfected cells;

however, these functions are impaired in CTBs infected with strain MR766.

Proliferating Amniotic Epithelial Cells Are Infected With American and African ZIKV Strains

Next, we determined whether ZIKV replicates in proliferating AmEpCs isolated from fetal membranes, as suggested by the patterns of PH3-positive cells and Ki67-positive infected CTBs and Hofbauer cells in anchoring villi. Many pairs and triplets of Nica1-16–infected AmEpCs expressed both NS3 and Ki67 (Figure 4A*i*) or PH3 (Figure 4A*ii*), indicating that the infected cells divided. Likewise, MR766-infected AmEpCs showed a similar configuration of PH3-positive infected cells (Figure 4A*iii*). To determine whether other ZIKV strains behave similarly, AmEpCs were also infected with the African ZIKV strain Dakar41519 (hereafter called Dakar) (Figure 4B*i,ii*), and PRVABC59, a contemporary American ZIKV strain from Puerto Rico (Figure 4B*iii,iv*). NS3 protein was detected in infected AmEpCs that also express PH3, indicating that the infected cells enter mitosis. We then determined whether TIM1, which serves as a cofactor for ZIKV infection [11], was expressed in proliferating AmEpCs. TIM1 was intensely stained in the plasma membranes and cytoplasm of uninfected cells, in pairs of mitotic cells and in Nica1-16–infected cells (Figure 4C*i,ii*).

To quantify the contribution of proliferating infected cells to overall ZIKV infection, we counted pairs and larger foci expressing E and NS3 in midgestation AmEpCs at 1 dpi

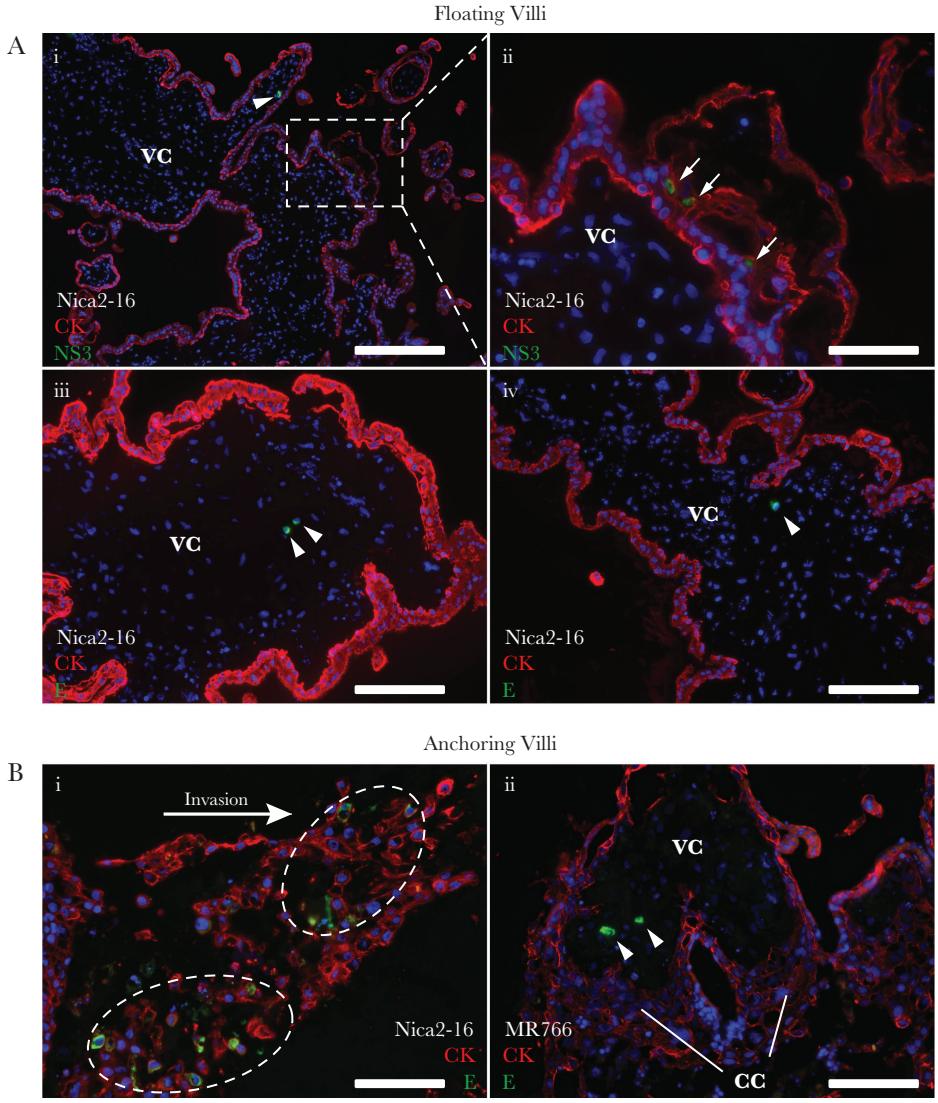

Figure 3. ZIKV infects Hofbauer cells and few CTBs in floating villus explants. Sections of floating (*A*) and anchoring villus explants from placenta 5 (*B*) infected with Nica2-16 or MR766 and immunostained for cytokeratin (CK) and ZIKV NS3 and E. *Ai, ii*, Nica2-16–infected cytotrophoblasts (CTBs, arrows) at a site of proliferation and (*Aiii, iv*) Nica2-16–infected Hofbauer cells (arrowheads) in villus cores (VC). *Bi*, Nica2-16–infected CTBs in a zone of invasive CTBs (dashed circles) in anchoring villi and (*ii*) MR766-infected Hofbauer cells (arrowheads) in villus core near a cell column (CC). Scale bars = 200 µm (*Ai*), 50 µm (*Aii*), and 100 µm (*Aiii, Aiv*, and *B*).

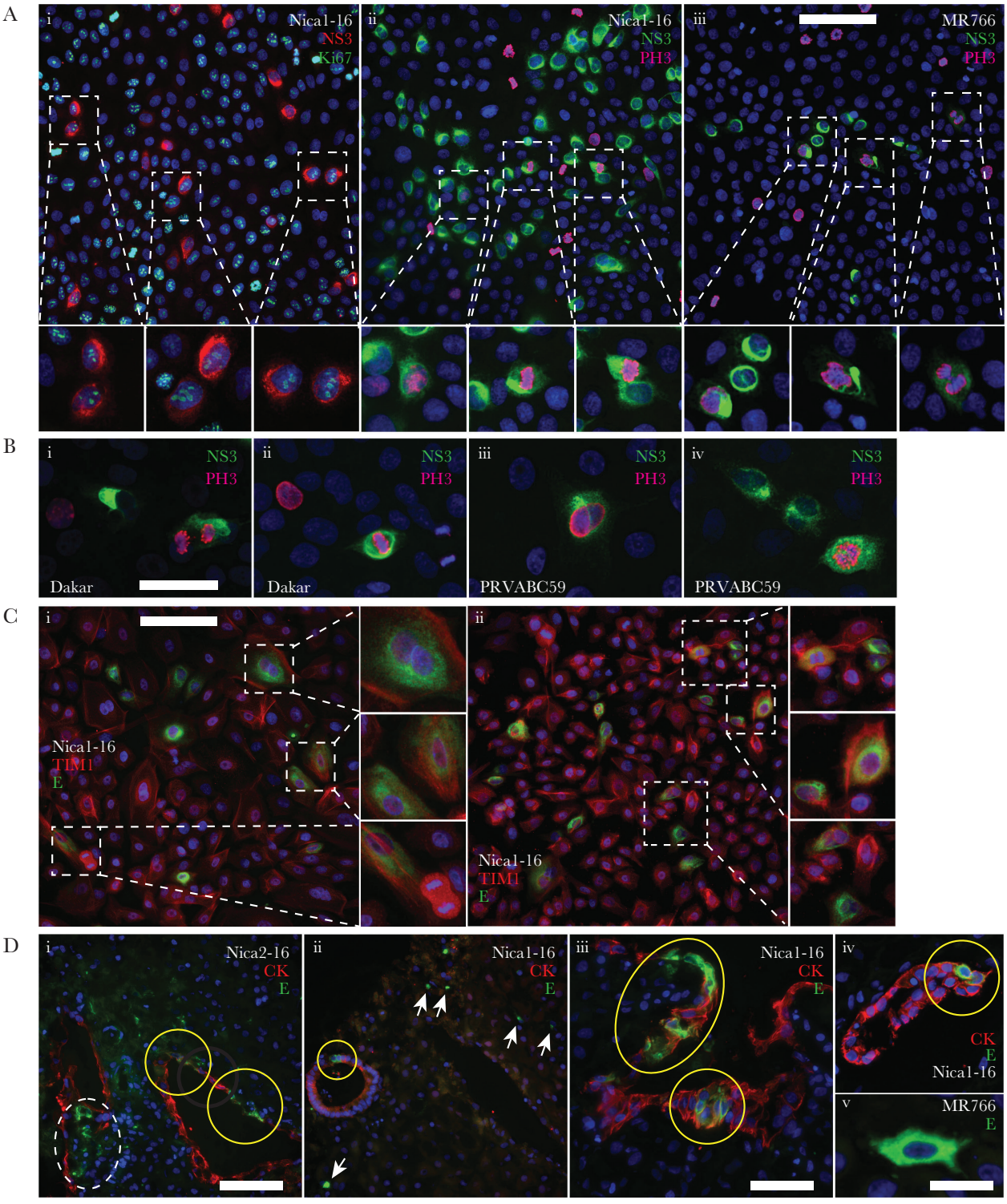

Figure 4. ZIKV replicates in midgestation amniotic epithelial cells that divide and glandular epithelium in basal decidua. *A*, Primary midgestation amniotic epithelial cells (AmEpCs) infected with Nica1-16 or MR766 and immunostained for ZIKV NS3 and either Ki67 (*i*) or phosphohistone H3 (PH3; *ii*, *iii*) at 1 day postinfection (dpi). Magnified images show infected cell pairs. *B*, Dakar- and PRVABC59-infected AmEpCs immunostained for NS3 and PH3. *C*, Nica1-16–infected AmEpCs immunostained for ZIKV E and TIM1 at 1 dpi showing infected cell pairs (magnified images). *D*, First-trimester basal decidua explants (n = 2) infected with Nica strains or MR766 and immunostained for cytokeratin (CK) and ZIKV E protein at 3 dpi. *Di–iv*, E protein detected in infected glandular epithelial cells immunostained for CK, and flanking stromal decidual cells. Yellow circles indicate infected glandular epithelial cells (*i–iv*) and dashed circle infected decidual cells (*i*, left). Arrows indicate infected immune cells (*ii*). *Dv*, An E protein-positive dendritic cell from MR766-infected decidua. Scale bars = 100 µm (*A*, *C*, *Di*, *ii*), 50 µm (*B*, *Diii*), and 20 µm (*v*).

Table 1. Reproducible Sites of Zika Virus Infection in Anchoring Villus Explants From First-Trimester Human Placentas

	Nica					MR766				
Placenta No.[a]	1	3	4	5	Totals Nica	7	6	3	5	Totals MR766
Gestational age (weeks)	8	10	11	11		7.5	8	10	11	
Anchoring villus sections[b,c]	41	10	42	150	243	44	11	8	49	112
Cell columns[d]	13/36 (36%)	1/4 (25%)	0/30 (0%)	3/69 (4%)	17/139 (12%)	18/35 (51%)	8/11 (73%)	5/10 (50%)	4/34 (12%)	35/90 (39%)
Zones of invasive CTBs[e]	31/35 (89%)	2/4 (50%)	16/24 (67%)	7/38 (18%)	56/101 (55%)	1/17 (6%)	1/11 (11%)	2/8 (25%)	0/23 (0%)	4/59 (7%)
Hofbauer cells in villus cores[d,f]	6/34 (18%)	4/6 (67%)	19/36 (53%)	24/67 (36%)	53/143 (37%)	10/40 (25%)	1/10 (10%)	0/11 (0%)	10/28 (36%)	21/89 (24%)

Abbreviations: CTB, cytotrophoblasts; NS3, nonstructural protein 3; ZIKV, Zika virus.

[a]Analysis of 6 placentas ranging in gestational age from 7.5 to 11 weeks, as indicated. Placenta numbers correspond to those presented in Supplementary Figure S1.

[b]All villi with positive immunostaining for ZIKV E and/or NS3 were examined for sites of infection. Numbers of villi showing infection at a given site are indicated relative to the number of infected villi examined.

[c]Analyzed at 3 days postinfection, 2 sections examined for most villi. Nica designates Nica1-16– and Nica2-16–infected explants.

[d]Proliferating CTBs in proximal cell columns.

[e]Zones refers to all invasive CTBs radiating from one villus. Differentiation/invasion of infected CTBs varied widely, with Nica-infected cells migrating more frequently and farther than MR766-infected cells (Figure 3). Infected zones were considered to be those with at least 5 infected CTBs.

[f]Infection of Hofbauer cells occurred in villus cores of both larger villi and smaller branching villi and was independent of nearby CTB infection (Figure 2).

(Supplementary Table S1). In Nica-infected AmEpCs at 19.4 weeks' gestation, 43.7% were in pairs and 1.7% in triplets. In Nica-infected AmEpCs at 21.2 weeks' gestation, 48.6% were pairs and 8.4% triplets. In MR766-infected AmEpCs, 60.4% were pairs and 2.7% were triplets. Moreover, 74% of infected cells in pairs expressed Ki67 as compared with 37% of single cells, suggesting a subset continued to divide.

To estimate the ability of African and American strains to replicate in midgestation AmEpCs, we compared the kinetics of production and titers of infectious progeny. The African prototype MR766 reached peak titers earlier than other ZIKV strains (Supplementary Figure S1), both African strains generated higher titers than the American strains Nica1-16 and PRVABC59, and Dakar-infected cells produced the highest virus titers. Together, these results showed that ZIKV replicates in proliferating AmEpCs expressing TIM1, increasing the population of infected cells, and the kinetics of viral replication are strain dependent.

DISCUSSION

In this study, we used low-multiplicity ZIKV infection to simulate maternal viremia associated with transplacental transmission [18, 25]. We showed that ZIKV infects consistent sites in anchoring villi and replicates in basal decidua from first-trimester human placentas, illustrated in a model of infection at the uterine–placental interface (Figure 6). ZIKV infects proliferating CTBs in cell columns that differentiate into invasive CTBs, as well as Hofbauer cells that proliferate in the villus core. We found that the frequency of infection at different sites depends on the virus strain. Furthermore, Nicaraguan ZIKV strains and the African prototype MR766 have different effects on CTB invasiveness, required for anchoring the placenta to the uterus. CTBs infected with Nicaraguan strains differentiated and invaded extracellular matrix, but MR766-infected cells were functionally impaired and largely restricted to foci of proliferating cells in proximal columns. High virus titers in anchoring villi correlated with numerous zones of Nica-infected invasive CTBs. In basal decidua, Nicaraguan strains infected glandular epithelium and dendritic cells and produced higher virus titers than MR766. ZIKV replication in decidua, also reported by others [26, 27], could contribute to infection of cell column CTBs by increasing the viral load in the interstitial blood space, and infected invasive CTBs could amplify infection in decidua. Pairs and triplets of infected AmEpCs expressing Ki67 or PH3 suggested that the number of proliferating ZIKV-infected cells increased in parallel with virus output. Likewise, proliferating infected Hofbauer cells could increase the viral load in villus cores, independent of CTB infection, and spread virus to the fetal circulation.

Analysis of numerous anchoring villus explants from first-trimester placentas confirms and extends the results of our published studies that CTBs and Hofbauer cells are targets of ZIKV infection [11]. Here we show that Nicaraguan ZIKV-infected CTBs proliferate, differentiate, and invade extracellular matrix alongside uninfected cells, thus generating a potential source of persistent viremia [7, 8]. The ability of Nica-infected cells to invade alongside uninfected cells implies that they express key molecules for invasion, cell–cell and cell–matrix adhesion receptors, possibly absent from MR766-infected CTBs [21]. However, MR766-infected cells express HLA-G [11], an unusual differentiation antigen whose transcripts accumulate in cell column CTBs well before the protein is made [28]. Whether MR766-infected CTBs have impaired de novo transcription of integrins required for invasion or whether reorganization

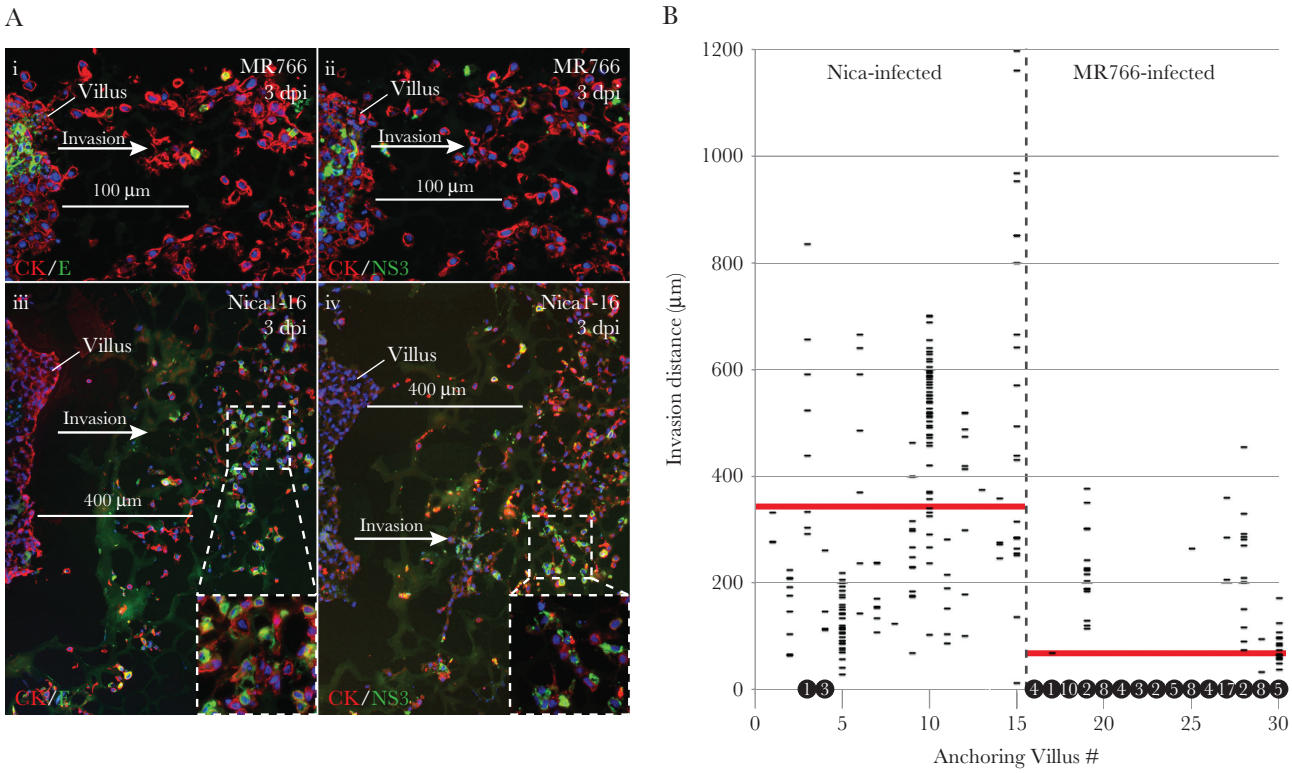

Figure 5. MR766 and Nica strains differentially affect CTB differentiation/invasion in anchoring villus explants. *A*, Adjacent sections of MR766-infected (*i, ii*) and Nica1-16–infected (*iii, iv*) anchoring villus explants immunostained for CK and either E (*i, iii*) or NS3 (*ii, iv*) at 3 days postinfection (dpi). *B*, Distances from villus tips of all infected cytotrophoblasts (CTBs) in sections of 15 MR766-infected and 15 Nica-infected anchoring villi at 3 dpi; horizontal lines represent individual infected CTBs. Numbers of infected CTBs remaining in cell columns (ie, migration distance = 0 µm) are indicated in black circles at y = 0; 4 Nica-infected and 83 MR766-infected cells were detected in cell columns. Red bars represent average invasion distance for each strain.

of microtubules into replication factories reduces invasiveness remains to be studied [29]. It is notable that Nica-infected explants develop robust zones of invasive CTBs and release infectious progeny. Interestingly, pathogenic strains of human cytomegalovirus (HCMV) infect proliferating CTBs in cell columns but upregulate viral and cellular factors that impair invasiveness [19, 30, 31]. Moreover, HCMV-infected AmEpCs proliferate and release low virus titers for months, suggesting persistent infection [20]. Processes that lead to transplacental transmission and contribute to pathology and fetal growth restriction in ZIKV-infected placentas, which differ from congenital HCMV infection, remain to be determined [1, 32–35].

The finding that ZIKV replicates in proliferating Hofbauer cells and AmEpCs has relevance for transmission and diagnosis of congenital infection. Analysis of a placenta from congenital ZIKV infection with microcephaly showed enlarged chorionic villi with extensive proliferation of Hofbauer cells in villus cores that were positive for ZIKV RNA [2, 36]. Moreover, ZIKV replicates in Hofbauer cells isolated from human placentas [26, 37]. Hofbauer cell proliferation increases during the first half of gestation, and these multifunctional, highly mobile cells have angiogenic properties, modulate villous branching and produce proinflammatory cytokines [24, 38–41]. Replication of ZIKV in proliferating AmEpCs also has implications for diagnosis of congenital infection by detection of viral RNA in amniotic fluid and inflammatory responses in the fetal compartment [42, 43]. However, some results could prove to be false negatives. For example, amniotic fluid from congenital ZIKV infection was positive when tested at midgestation, but negative when retested later in pregnancy [8]. Likewise, we found that ZIKV titers were reduced in AmEpCs from third-trimester placentas, suggesting slowed proliferation contributes to negative results later in pregnancy [11].

How ZIKV breaches the protective architecture of chorionic villi is puzzling, considering that infection of Hofbauer cells in villus cores occurs without nearby simultaneous CTB infection. Recently, mutations in the nonstructural protein (NS1) were shown to enhance ZIKV infectivity in mosquitoes [44]. Possibly, NS1 virus stocks enhance infection of villus explants. NS1 disrupts the glycocalyx on the surface of endothelial cells, leading to endothelial hyperpermeability [45] and might perturb the loosely associated cell column CTBs by cleaving proteoglycans in the glycocalyx, thereby increasing permeability and providing virus access to Hofbauer cells, where locally produced NS1 in villus cores could facilitate ZIKV transmission across the endothelium to fetal circulation. NS1 of American strains contains an intertwined loop that forms a hydrophobic

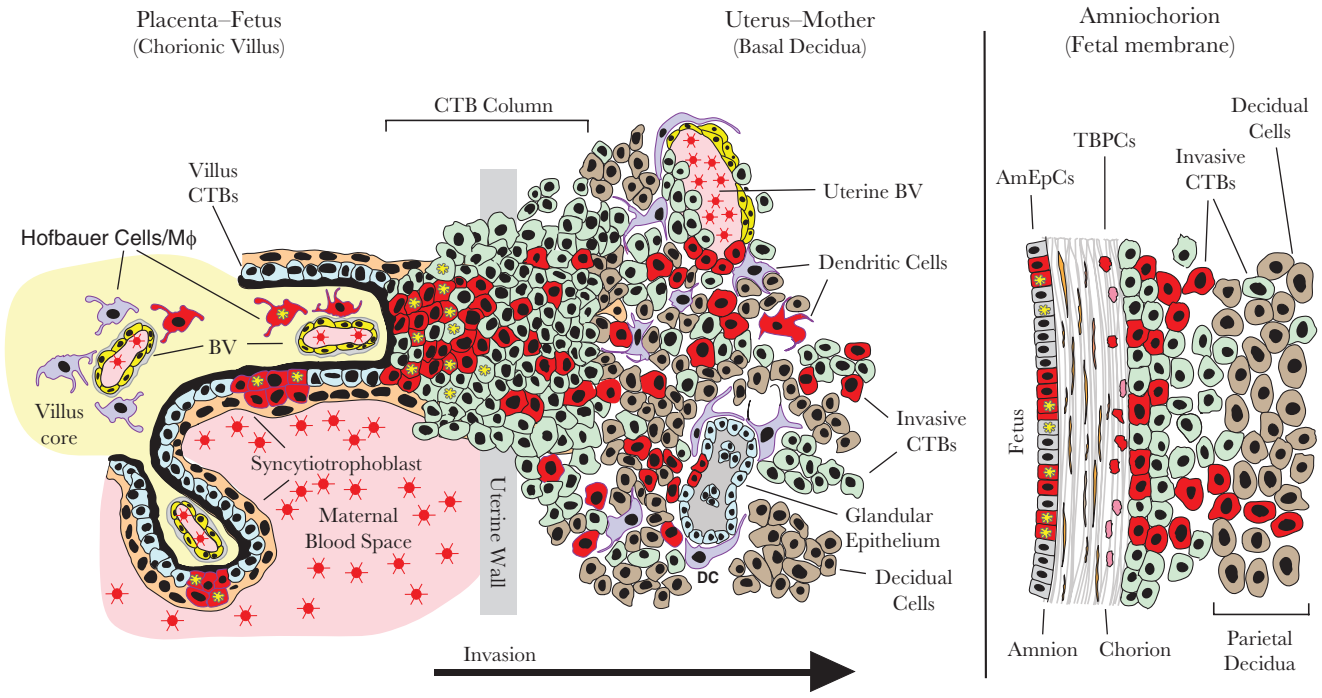

Figure 6. Model of ZIKV infection at the uterine–placental interface. Left panel, in the placenta, ZIKV replicates in proliferating cytotrophoblasts in cell columns that differentiate, invade the basal decidua and remodel uterine blood vessels, and in Hofbauer cells in the villus core [11]. In basal decidua, ZIKV replicates in glandular epithelial cells, decidual cells, and dendritic cells. Right panel, ZIKV infects amniotic epithelial cells that proliferate in the amniotic membrane and trophoblast progenitor cells in the chorionic membrane that differentiate into cytotrophoblasts and infiltrate the parietal decidua [48, 49]. Red cytoplasm represents ZIKV-infected cells; red "stars" represent virions; yellow serrated nuclei represent proliferating cells. Abbreviations: CTBs, cytotrophoblasts; MΦ, macrophage; BV, blood vessel; AmEpCs, amniotic epithelial cells; TBPCs, trophoblast progenitor cells.

spike, thought to contribute to membrane association, which is not present in NS1 of dengue or West Nile viruses [46]. NS1 could also trigger innate immune responses, leading to release of proinflammatory cytokines [47]. Together, our results show that ZIKV replicates in anchoring villi and basal decidua from first-trimester placentas, generating a source of prolonged viremia during early development, leading to transplacental transmission.

Supplementary Data

Supplementary materials are available at *The Journal of Infectious Diseases* online. Consisting of data provided by the authors to benefit the reader, the posted materials are not copyedited and are the sole responsibility of the authors, so questions or comments should be addressed to the corresponding author.

Notes

Acknowledgments. We thank June Fang-Hoover for technical assistance and Michael Diamond for ZIKV strains. We appreciate discussions with Chunling Wang and Daniel W. Gerlich.

Financial support. This work was supported by grants from the NIH Institute for Allergy and Infectious Diseases: RO1AI04667 (L. P.), R21 AI129508 (L. P., E. H.), and RO1AI124493 (E. H.).

Potential conflicts of interest. All authors: No reported conflicts of interest. All authors have submitted the ICMJE Form for Disclosure of Potential Conflicts of Interest. Conflicts that the editors consider relevant to the content of the manuscript have been disclosed.

References

1. Melo AS, Aguiar RS, Amorim MM, et al. Congenital Zika virus infection: beyond neonatal microcephaly. JAMA Neurol **2016**; 73:1407–16.
2. Brasil P, Pereira JP Jr, Moreira ME, et al. Zika virus infection in pregnant women in Rio de Janeiro. N Engl J Med **2016**; 375:2321–34.
3. Mlakar J, Korva M, Tul N, et al. Zika virus associated with microcephaly. N Engl J Med **2016**; 374:951–8.
4. Rasmussen SA, Jamieson DJ, Honein MA, Petersen LR. Zika virus and birth defects–reviewing the evidence for causality. N Engl J Med **2016**; 374:1981–7.
5. van der Linden V, Pessoa A, Dobyns W, et al. Description of 13 infants born during October 2015-January 2016 with congenital Zika virus infection without microcephaly at birth—Brazil. MMWR Morb Mortal Wkly Rep **2016**; 65:1343–8.
6. Fajardo Á, Cristina J, Moreno P. Emergence and spreading potential of Zika virus. Front Microbiol **2016**; 7:1667.

7. Driggers RW, Ho CY, Korhonen EM, et al. Zika virus infection with prolonged maternal viremia and fetal brain abnormalities. N Engl J Med **2016**; 374:2142–51.
8. Schaub B, Vouga M, Najioullah F, et al. Analysis of blood from Zika virus-infected fetuses: a prospective case series. Lancet Infect Dis **2017**; 17:520–7.
9. Weaver SC, Costa F, Garcia-Blanco MA, et al. Zika virus: history, emergence, biology, and prospects for control. Antiviral Res **2016**; 130:69–80.
10. Lazear HM, Diamond MS. Zika virus: new clinical syndromes and its emergence in the Western Hemisphere. J Virol **2016**; 90:4864–75.
11. Tabata T, Petitt M, Puerta-Guardo H, et al. Zika virus targets different primary human placental cells, suggesting two routes for vertical transmission. Cell Host Microbe **2016**; 20:155–66.
12. Prakobphol A, Genbacev O, Gormley M, Kapidzic M, Fisher SJ. A role for the L-selectin adhesion system in mediating cytotrophoblast emigration from the placenta. Dev Biol **2006**; 298:107–17.
13. Genbacev OD, Prakobphol A, Foulk RA, et al. Trophoblast L-selectin-mediated adhesion at the maternal-fetal interface. Science **2003**; 299:405–8.
14. Zhou Y, Fisher SJ, Janatpour M, et al. Human cytotrophoblasts adopt a vascular phenotype as they differentiate. A strategy for successful endovascular invasion? J Clin Invest **1997**; 99:2139–51.
15. Librach CL, Werb Z, Fitzgerald ML, et al. 92-kD type IV collagenase mediates invasion of human cytotrophoblasts. J Cell Biol **1991**; 113:437–49.
16. McMaster MT, Librach CL, Zhou Y, et al. Human placental HLA-G expression is restricted to differentiated cytotrophoblasts. J Immunol **1995**; 154:3771–8.
17. Castellucci M, Kosanke G, Verdenelli F, Huppertz B, Kaufmann P. Villous sprouting: fundamental mechanisms of human placental development. Hum Reprod Update **2000**; 6:485–94.
18. Waggoner JJ, Gresh L, Vargas MJ, et al. Viremia and clinical presentation in nicaraguan patients infected with Zika virus, Chikungunya virus, and Dengue virus. Clin Infect Dis **2016**; 63:1584–90.
19. Tabata T, Petitt M, Fang-Hoover J, et al. Cytomegalovirus impairs cytotrophoblast-induced lymphangiogenesis and vascular remodeling in an in vivo human placentation model. Am J Pathol **2012**; 181:1540–59.
20. Tabata T, Petitt M, Fang-Hoover J, Zydek M, Pereira L. Persistent cytomegalovirus infection in amniotic membranes of the human placenta. Am J Pathol **2016**; 186:2970–86.
21. Damsky CH, Fitzgerald ML, Fisher SJ. Distribution patterns of extracellular matrix components and adhesion receptors are intricately modulated during first trimester cytotrophoblast differentiation along the invasive pathway, in vivo. J Clin Invest **1992**; 89:210–22.
22. Balsitis SJ, Coloma J, Castro G, et al. Tropism of dengue virus in mice and humans defined by viral nonstructural protein 3-specific immunostaining. Am J Trop Med Hyg **2009**; 80:416–24.
23. Henchal EA, Gentry MK, McCown JM, Brandt WE. Dengue virus-specific and flavivirus group determinants identified with monoclonal antibodies by indirect immunofluorescence. Am J Trop Med Hyg **1982**; 31:830–6.
24. Castellucci M, Celona A, Bartels H, Steininger B, Benedetto V, Kaufmann P. Mitosis of the Hofbauer cell: possible implications for a fetal macrophage. Placenta **1987**; 8:65–76.
25. Musso D, Roche C, Nhan TX, Robin E, Teissier A, Cao-Lormeau VM. Detection of Zika virus in saliva. J Clin Virol **2015**; 68:53–5.
26. El Costa H, Gouilly J, Mansuy JM, et al. ZIKA virus reveals broad tissue and cell tropism during the first trimester of pregnancy. Sci Rep **2016**; 6:35296.
27 . Weisblum Y, Oiknine-Djian E, Vorontsov OM, et al. Zika virus infects early- and midgestation human maternal decidual tissues, inducing distinct innate tissue responses in the maternal-fetal interface. J Virol **2017**; 91:e01905–16.
28. Copeman J, Han RN, Caniggia I, McMaster M, Fisher SJ, Cross JC. Posttranscriptional regulation of human leukocyte antigen G during human extravillous cytotrophoblast differentiation. Biol Reprod **2000**; 62:1543–50.
29. Cortese M, Goellner S, Acosta EG, et al. Ultrastructural characterization of Zika virus replication factories. Cell Rep **2017**; 18:2113–23.
30. Tabata T, McDonagh S, Kawakatsu H, Pereira L. Cytotrophoblasts infected with a pathogenic human cytomegalovirus strain dysregulate cell-matrix and cell-cell adhesion molecules: a quantitative analysis. Placenta **2007**; 28:527–37.
31. Yamamoto-Tabata T, McDonagh S, Chang HT, Fisher S, Pereira L. Human cytomegalovirus interleukin-10 downregulates metalloproteinase activity and impairs endothelial cell migration and placental cytotrophoblast invasiveness in vitro. J Virol **2004**; 78:2831–40.
32. Pereira L, Petitt M, Fong A, et al. Intrauterine growth restriction caused by underlying congenital cytomegalovirus infection. J Infect Dis **2014**; 209:1573–84.
33. Nozawa N, Fang-Hoover J, Tabata T, Maidji E, Pereira L. Cytomegalovirus-specific, high-avidity IgG with neutralizing activity in maternal circulation enriched in the fetal bloodstream. J Clin Virol **2009**; 46(Suppl 4):S58–63.
34. Tabata T, Petitt M, Zydek M, et al. Human cytomegalovirus infection interferes with the maintenance and differentiation of trophoblast progenitor cells of the human placenta. J Virol **2015**; 89:5134–47.
35. Tabata T, Kawakatsu H, Maidji E, et al. Induction of an epithelial integrin alphavbeta6 in human cytomegalovirus-infected

endothelial cells leads to activation of transforming growth factor-beta1 and increased collagen production. Am J Pathol **2008**; 172:1127–40.
36. Rosenberg AZ, Yu W, Hill DA, Reyes CA, Schwartz DA. Placental pathology of Zika virus: viral infection of the placenta induces villous stromal macrophage (Hofbauer cell) proliferation and hyperplasia. Arch Pathol Lab Med **2017**; 141:43–8.
37. Quicke KM, Bowen JR, Johnson EL, et al. Zika virus infects human placental macrophages. Cell Host Microbe **2016**; 20:83–90.
38. Ingman K, Cookson VJ, Jones CJ, Aplin JD. Characterisation of Hofbauer cells in first and second trimester placenta: incidence, phenotype, survival in vitro and motility. Placenta **2010**; 31:535–44.
39. Seval Y, Korgun ET, Demir R. Hofbauer cells in early human placenta: possible implications in vasculogenesis and angiogenesis. Placenta **2007**; 28:841–5.
40. Anteby EY, Natanson-Yaron S, Greenfield C, et al. Human placental Hofbauer cells express sprouty proteins: a possible modulating mechanism of villous branching. Placenta **2005**; 26:476–83.
41. Young OM, Tang Z, Niven-Fairchild T, et al. Toll-like receptor-mediated responses by placental Hofbauer cells (HBCs): a potential pro-inflammatory role for fetal M2 macrophages. Am J Reprod Immunol **2015**; 73:22–35.
42. Calvet G, Aguiar RS, Melo ASO, et al. Detection and sequencing of Zika virus from amniotic fluid of fetuses with microcephaly in Brazil: a case study. Lancet Infect Dis **2016**; 16:653–60.
43. Ornelas AM, Pezzuto P, Silveira PP, et al. Immune activation in amniotic fluid from Zika virus-associated microcephaly. Ann Neurol **2017**; 81:152–6.
44. Liu Y, Liu J, Du S, et al. Evolutionary enhancement of Zika virus infectivity in *Aedes aegypti* mosquitoes. Nature **2017**; 545:482–6.
45. Puerta-Guardo H, Glasner DR, Harris E. Dengue virus NS1 disrupts the endothelial glycocalyx, leading to hyperpermeability. PLoS Pathog **2016**; 12:e1005738.
46. Xu X, Song H, Qi J, et al. Contribution of intertwined loop to membrane association revealed by Zika virus full-length NS1 structure. EMBO J **2016**; 35:2170–8.
47. Modhiran N, Watterson D, Muller DA, et al. Dengue virus NS1 protein activates cells via Toll-like receptor 4 and disrupts endothelial cell monolayer integrity. Sci Transl Med **2015**; 7:304ra142.
48. Genbacev O, Donne M, Kapidzic M, et al. Establishment of human trophoblast progenitor cell lines from the chorion. Stem Cells **2011**; 29:1427–36.
49. Genbačev O, Vićovac L, Larocque N. The role of chorionic cytotrophoblasts in the smooth chorion fusion with parietal decidua. Placenta **2015**; 36:716–22.